

ChemComm

Accepted Manuscript



This is an *Accepted Manuscript*, which has been through the Royal Society of Chemistry peer review process and has been accepted for publication.

Accepted Manuscripts are published online shortly after acceptance, before technical editing, formatting and proof reading. Using this free service, authors can make their results available to the community, in citable form, before we publish the edited article. We will replace this *Accepted Manuscript* with the edited and formatted *Advance Article* as soon as it is available.

You can find more information about *Accepted Manuscripts* in the [Information for Authors](#).

Please note that technical editing may introduce minor changes to the text and/or graphics, which may alter content. The journal's standard [Terms & Conditions](#) and the [Ethical guidelines](#) still apply. In no event shall the Royal Society of Chemistry be held responsible for any errors or omissions in this *Accepted Manuscript* or any consequences arising from the use of any information it contains.



ChemComm

COMMUNICATION

Visualization of ion transport in Nafion using electrochemical strain microscopy

Received 00th January 20xx,
Accepted 00th January 20xx

Suran Kim,^{ab} Kwangsoo No^{*b} and Seungbum Hong^{*ab}

DOI: 10.1039/x0xx00000x

www.rsc.org/

The electromechanical response of a Nafion membrane immersed in water was probed using electrochemical strain microscopy (ESM) to redistribute protons and measure the resulting local strain that is caused by the movement of protons. We also measured the relaxation of protons from the surface resulting from proton diffusion. Using this technique, we can visualize and analyze the local strain change resulting from the redistribution and relaxation of hydrated protons.

Nafion membranes are complex ion-conducting materials that have been widely used in various fields from energy applications^{1,2}, including fuel cells and energy harvesting, to bio-inspired and biomedical applications³⁻⁶, such as active catheter systems, heart-assistive devices, and artificial muscles. Nafion consists of a perfluorinated backbone polymer with side-chains containing negatively charged sulfonic end groups. When hydrated, sulfonic acid groups segregate from the hydrophobic backbone and form an ionic conductive water-filled network that allows transport of ions and water. Nafion shows high proton conductivity, selective permeability to water, and excellent chemical stability.^{2,7} Proton conductivity is an important factor for high functionality, and it depends on the nanostructure inside the membranes and the proton transport behaviour through the membranes.⁸

Many groups have investigated the macroscopic proton conductivity of Nafion using ac impedance spectroscopy, dc techniques, and current pulse technique to understand the transport mechanism and find more efficient morphologies for higher proton conductivity.⁹⁻¹² The proton conductivity has been studied under various conditions including humidity, temperature, and pressure.^{10,11} It was shown that the proton conductivity of Nafion highly depends on the humidity and heat-treatment of the membrane.¹⁰ The Okada group found that the specific conductivity of the membrane is determined by the interaction of ions with

water and the microscopic membrane channel structure such as the ionic domain shape and size and the inter-connectivity of the domains as well as the mobility of the ions.¹² Although macroscopic measurement has provided useful insight into the proton transport mechanism, it has offered limited information about the local variations of proton conductivity on a nanoscale,¹³ which result from the density and distribution of ionic domains.

Atomic force microscopy (AFM) based techniques have been applied to probe local conductivity and the density and distribution of ionic domains. By contacting the film surface with the conductive AFM tip and applying bias across the membrane, one can measure and analyse the local currents that are produced by both ionic and electronic currents inside the membrane and electrochemical reactions at the tip/membrane interface.¹³⁻¹⁷ Rumberger and his co-worker recently studied nanoscale surface-potential fluctuation in thin films of low-hydrated Nafion using non-contact electrostatic force microscopy (EFM).¹⁸ They found that the observed fluctuations are produced by water-facilitated hydrogen-ion hopping within the ion channel network.

To visualize and analyse proton transport behaviour and to decouple the proton transport from the electronic current, we used electrochemical strain microscopy (ESM) techniques. ESM is a technique that measures the bias-induced strain change on a surface caused by the ion transport and accompanying intercalation and extraction of the ions, usually in a solid electrolyte material using a conductive AFM tip. In recent years, ESM techniques have been widely used in Li-conducting ceramics for Li-ion batteries¹⁹⁻²⁵ but have not yet been applied to ion-conducting polymers such as Nafion. As Nafion also shows an electromechanical response due to the movement of hydrated protons and the local strain is caused by only ions and hydrated ions, we can visualize and analyse the local proton transport behaviour using ESM.

Here, we measured the ESM response of a Nafion surface immersed in deionized water while applying both ac and dc voltages to the ESM tip on Nafion surface. In addition, we measured the relaxation of the ions from the surface by repeating ESM imaging on the same regions that were biased by either positive or negative dc bias voltages.

^a Material Science Division, Argonne National Laboratory, Lemont, 60439, IL, USA.
E-mail: hong@anl.gov

^b Department of Material Science and Engineering, KAIST, Daejeon, 305-701, Korea. E-mail: ksno@kaist.ac.kr

† Electronic Supplementary Information (ESI) available: Details of ESM image in ambient and water conditions. See DOI: 10.1039/x0xx00000x

COMMUNICATION

ChemComm

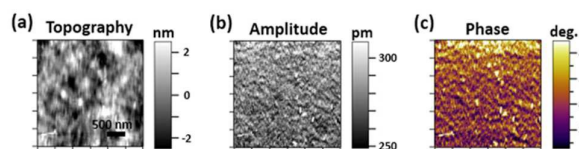


Fig. 1 ESM of Nafion in a water condition; (a) topography (b) amplitude and (c) phase of ESM response.

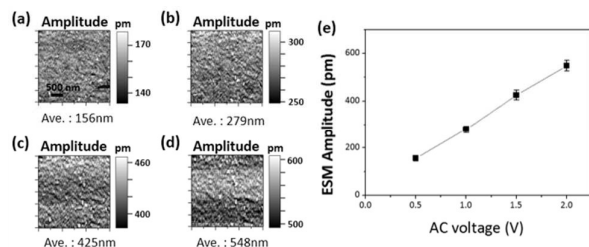


Fig. 2 ESM amplitude images under different ac voltages of (a) 0.5 V_{ac} , (b) 1 V_{ac} , (c) 1.5 V_{ac} , and (d) 2 V_{ac} . (e) shows the relationship between ESM amplitude and V_{ac} .

First, we observed the electromechanical response of Nafion in a water environment using ESM, as shown in Fig. 1. The surface roughness was 1.2 nm over a 3 μm by 3 μm area measured from Fig. 1a. The ESM amplitude in Fig. 1b represents the high frequency (~ 100 kHz) motion of protons, induced by the ac bias via the AFM tip, which was 279 pm/V \pm 14.6 pm/V. The ESM phase shows the delay of the motion of protons, which is around 41.4 degrees, as shown in Fig. 1c. In the case of single frequency ESM, the phase can either increase or decrease if the contact resonance frequency changes due to the change in the elastic constant of the surface.²⁶ However, we used DART ESM, which tracks the resonance frequency in real-time. Therefore, the ESM phase will only change if the surface damping changes. The phase will increase when the damping constant increases as it broadens the resonance ESM peak, as shown in Fig. S6 (ESI[†]).^{27–29} Similar to piezoresponse force microscopy (PFM), the ESM tip creates a highly non-uniform ac electric field near the tip when the capacitive component of Nafion

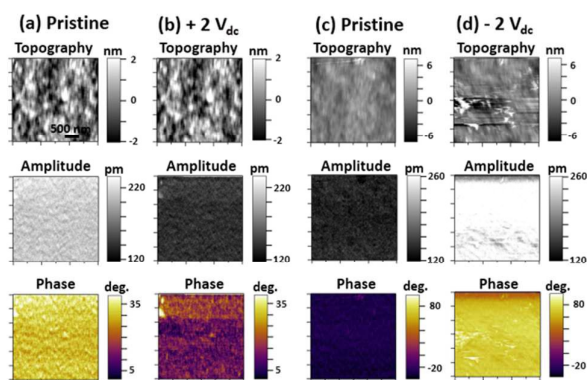
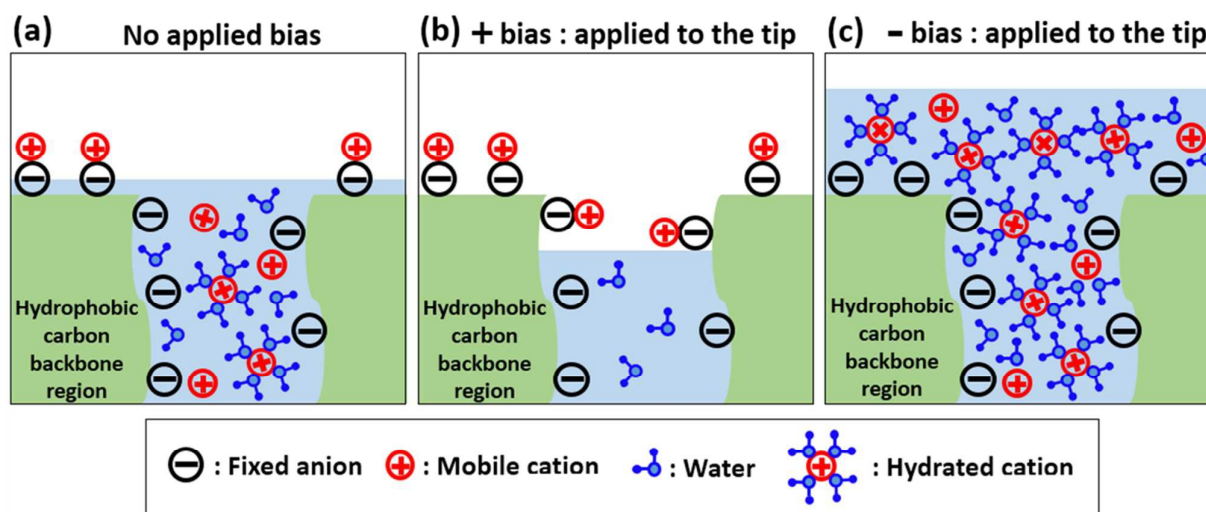


Fig. 3 Topography (upper), ESM amplitude (middle), and ESM phase (lower) images of pristine state (a, c) and while applying (b) +2 V_{dc} and (d) -2 V_{dc} to tip.

increases at high frequency and a higher electric field concentrates on the surface of the Nafion membrane.³⁰ As such, the net motion of protons will increase under the same ac field as the protons move closer to the surface.

The bias-induced proton movement under an electric field includes diffusion and electro-migration.³¹ As we apply a higher ac electric field to the sample, the protons fluctuate more rapidly because the proton flux is proportional to the amplitude of the electric field, which will increase the ESM amplitude. Indeed, the ESM amplitude linearly increased with the ac voltage from 0.5 to 2.0 V_{ac} as shown in Fig. 2e. This linear relationship suggests that the motion of protons did not involve any irreversible component such as diffusion from one site to the other.³²

To observe the ion redistribution under electrical stimulation, $\pm 2 V_{dc}$ was applied to the tip while scanning the whole area. We compared the topography and ESM images of the pristine region before and while applying the dc bias voltage, as shown in Fig. 3. As the polarity of the electric force gradient is expected to change depending on the proton concentration near the surface, the ESM



Scheme 1 Schematic configurations of protons, fixed anions, and water near the surface of the Nafion membrane with (a) no applied bias and (b) positive and (c) negative voltages applied to the tip.

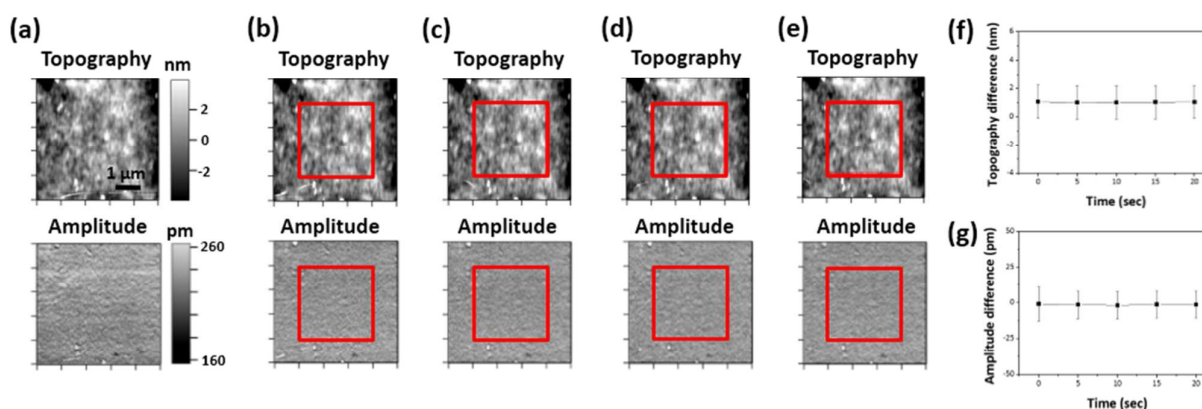


Fig. 4 Topography (upper) and ESM amplitude (lower) images of (a) pristine state and after applying +2 V_{dc} for (b) 5 min, (c) 10 min, (d) 15 min, and (e) 20 min (red box: the region where we applied +2 V_{dc}). Plots of (f) net topography difference and (g) net ESM amplitude as a function of the elapsed time after the bias application

phase will change in the opposite direction if we change the polarity of the dc bias. The ESM amplitude increased as we applied negative dc bias whereas it decreased when we applied positive bias, which is in agreement with the hypothesis that more protons near the surface will contribute to higher ESM amplitude. While the topography remained almost unchanged when we applied the positive bias, the topography showed a locally swollen surface when we applied negative bias to the tip, as shown in Fig. 3d. The change in the surface morphology was well reflected in the overall surface roughness (3.494 nm) of a negatively biased region, which showed almost a three times higher value than that (1.209 nm) of the pristine region.

To explain these results, we provide a schematic configuration of protons, fixed anions, and water near the surface of the Nafion membrane with (a) no applied bias and (b) positive and (c) negative voltages applied to the tip, as shown in Scheme 1. The microstructure of Nafion consists of a hydrophobic carbon backbone and hydrophilic regions. The hydrophilic region contains hydrated protons, water, and protons, as schematically illustrated in Scheme 1a.

If positive bias voltage is applied to the tip, the hydrated protons move towards the bottom electrode whereas the hydrophobic region remains intact, which is illustrated in Scheme

1b. With positive bias voltage applied to the tip, therefore, the ESM amplitude decreased while the topography showed no changes, as presented in Figs. 3a, b.

In the case of negative bias voltage, hydrated protons migrate to the tip, as shown in Scheme 1c. Since we obtained the ESM membrane in a water environment, there was sufficient water to move toward the tip from the surroundings. The hydrated protons will be temporarily adsorbed on the surface of the hydrophobic region. Therefore, the ESM amplitude increased and the surface topography shows a swollen surface when we applied negative bias voltage to the tip, which is supported by Figs. 3c, d. A large number of hydrated protons appear to form a continuous layer on the surface of the hydrophobic region, which contributes to the swollen surface morphology as seen in Fig. 3d.

To observe the time and bias polarity dependence of the ion transport behaviour after the application of bias voltage, we observed the change of the topography and ESM amplitude after applying +2 V_{dc} and -2 V_{dc} to the ESM tip. We focused on the ESM amplitude because this parameter and the phase show similar behaviour and the proton relaxation is the phenomenon that we are interested in. To observe the ESM amplitude contrast and facilitate a comparison between different regions in Figs. 4 and 5, we subtracted the background using the ImageJ program (National

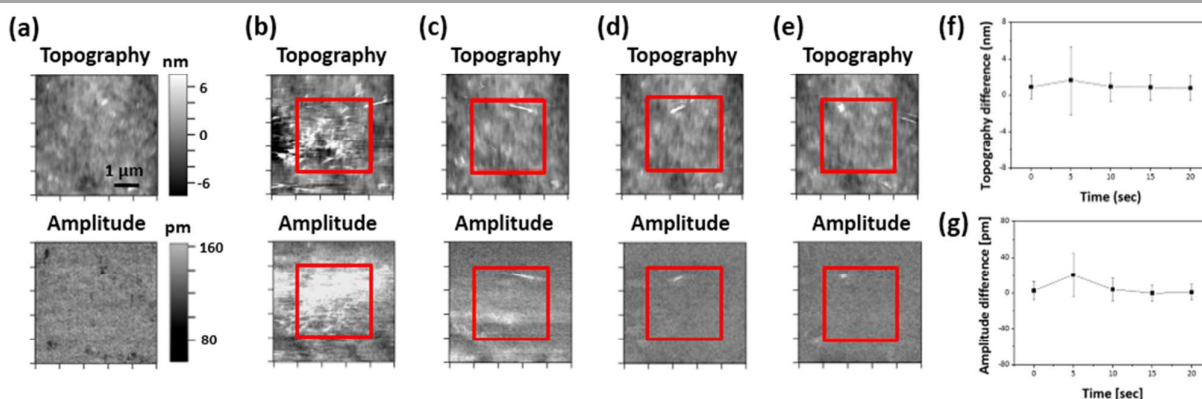


Fig. 5 Topography (upper) and ESM amplitude (lower) images of (a) pristine state and after applying -2 V_{dc} for (b) 5 min, (c) 10 min, (d) 15 min, and (e) 20 min (red box: the region where we applied -2 V_{dc}). Plots of (f) net height difference and (g) net ESM amplitude as a function of the elapsed time after the bias application.

Institute of Health). The raw images for both ESM amplitude and phase images for Figs. 4 and 5 are presented in the supplementary information (see Figs. S4 and S5, ESI†).

First, we compared the topography and ESM amplitude of the pristine region before and after applying $+2 V_{dc}$ as a function of the elapsed time after the bias application, as shown in Figs. 4a-e. As it was difficult to detect any differences between the pristine and the biased regions, we plotted the net height difference as well as the net ESM amplitude in the electrically biased area versus time, where the net height difference and the net ESM amplitude refer to the average topography height and the ESM amplitude of the electrically biased region (red box) at the time of interest subtracted by the average value of the topography height and the ESM amplitude of the pristine region, respectively. Figs. 4f-g plot the net height difference and the net ESM amplitude as functions of the elapsed time after bias application, which show very little change over the full range of the elapsed time.

Second, we compared the topography and the ESM amplitude of the pristine region before and after applying $-2 V_{dc}$ as a function of the elapsed time after the bias application, as shown in Fig. 5. From Fig. 5b, we found that the surface topography underwent local changes as evidenced by the randomly clustered white features within the region where bias voltage was applied. These topography changes were accompanied by local ESM amplitude changes as well, although the region affected in ESM was larger than that in the topography. This indicates that the topography change may occur after a sufficient number of ions move to the surface. We also found that there is a spatial distribution of the local topography changes due to inhomogeneous nanostructures of Nafion. As the time elapsed, the swollen surface returned to the original morphology and the amplitude distribution also returned close to the original state, as shown in Fig. 5, which is due to the diffusion of electrically stimulated protons in the swollen region.

In summary, we demonstrated that the proton distribution and the transport behaviour in an ionic polymer could be visualized using strain detection in ESM. We observed the local strain caused only by the movement of hydrated protons in Nafion immersed in deionized water. When electrically stimulated by an AFM tip, the hydrated protons moved toward the cathode and induced strain. Immediately after being electrically stimulated by the AFM tip, these hydrated protons diffused out due to the concentration distribution. We also found that this transport behaviour of hydrated protons is asymmetric between positive and negative voltage cases. Moreover, we obtained quantitative information about the local strain and proton diffusion. The ESM approach in our study shows how the local strain is induced by the proton transport behaviour, which is considered an important factor for designing polymer electrolyte materials. We believe that our study will be invaluable for investigating and improving the performance of these materials in various applications, including fuel cells and artificial muscles.

Acknowledgments

The work was supported by the U.S. Department of Energy, Office of Science, Materials Sciences and Engineering Division. S.K. acknowledges support from Brain Korea 21 Plus and KAIST

for the guest graduate student program at Argonne National Laboratory.

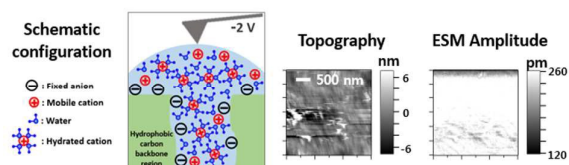
Notes and references

- 1 L. Carrette, K. A. Friedrich and U. Stimming, *Fuel Cells*, 2001, **1**, 5–39.
- 2 O. Savadogo, *J. New Mat. Electrochem. Syst.*, 1998, **1**, 47–66.
- 3 J. Kim, J. H. Jeon, H. J. Kim, H. Lim and I. K. Oh, *ACS Nano*, 2014, **8**, 2986–2997.
- 4 S. Liu, Y. Liu, H. Cebeci, R. G. De Villoria, J. H. Lin, B. L. Wardle and Q. M. Zhang, *Adv. Funct. Mater.*, 2010, **20**, 3266–3271.
- 5 R. Tiwari and E. Garcia, *Smart Mater. Struct.*, 2011, **20**, 083001.
- 6 S. Kim, S. Hong, Y. Y. Choi, H. Song and K. No, *Electrochim. Acta*, 2013, **108**, 547–553.
- 7 O. Savadogo, *J. Power Sources*, 2004, **127**, 135–161.
- 8 K. A. Mauritz and R. B. Moore, *Chem. Rev.*, 2004, **104**, 4535–4585.
- 9 M. W. Verbrugge and R. F. Hill, *J. Electrochem. Soc.*, 1990, **137**, 3770.
- 10 Y. Sone, P. Ekdunge and D. Simonsson, *J. Electrochem. Soc.*, 1996, **143**, 1254.
- 11 F. N. Büchi and G. G. Scherer, *J. Electroanal. Chem.*, 1996, **404**, 37–43.
- 12 T. Okada, G. Xie, O. Gorseth, S. Kjelstrup, N. Nakamura and T. Arimura, *Electrochim. Acta*, 1998, **43**, 3741–3747.
- 13 R. Hiesgen, E. Aleksandrova, G. Meichsner, I. Wehl, E. Roduner and K. A. Friedrich, *Electrochim. Acta*, 2009, **55**, 423–429.
- 14 E. Aleksandrova, R. Hiesgen, K. A. Friedrich and E. Roduner, *Phys. Chem. Chem. Phys.*, 2007, **9**, 2735–2743.
- 15 D. A. Bussian, J. R. O'Dea, H. Metiu and S. K. Buratto, *Nano Lett.*, 2007, **7**, 227–232.
- 16 E. Aleksandrova, S. Hink, R. Hiesgen and E. Roduner, *J. Phys. Condens. Matter*, 2011, **23**, 234109.
- 17 A. N. Morozovska, E. A. Eliseev and S. V. Kalinin, *Appl. Phys. Lett.*, 2010, **96**, 222906.
- 18 B. Rumberger, M. Bennett, J. Zhang, J. A. Dura and N. E. Israeloff, *J. Chem. Phys.*, 2014, **141**, 071102.
- 19 N. Balke, S. Jesse, A. N. Morozovska, E. Eliseev, D. W. Chung, Y. Kim, L. Adamczyk, R. E. García, N. Dudney and S. V. Kalinin, *Nanotechnol.*, 2010, **5**, 749–754.
- 20 N. Balke, S. Jesse, Y. Kim, L. Adamczyk, A. Tselev, I. N. Ivanov, N. J. Dudney and S. V. Kalinin, *Nano Lett.*, 2010, **10**, 3420–3425.
- 21 N. Balke, S. Jesse, Y. Kim, L. Adamczyk, I. N. Ivanov, N. J. Dudney and S. V. Kalinin, *ACS Nano*, 2010, **4**, 7349–7357.
- 22 T. M. Arruda, A. Kumar, S. V. Kalinin and S. Jesse, *Nano Lett.*, 2011, **11**, 4161–4167.
- 23 J. A. A. W. Elemans, *Nat. Chem.*, 2011, **3**, 656–657.
- 24 S. Kalinin, N. Balke, S. Jesse, A. Tselev, A. Kumar, T. M. Arruda, S. Guo and R. Proksch, *Mater. Today*, 2011, **14**, 548–558.
- 25 Q. N. Chen, Y. Ou, F. Ma and J. Li, *Appl. Phys. Lett.*, 2014, **104**, 242907.
- 26 S. Jesse, B. Mirman and S. V. Kalinin, *Appl. Phys. Lett.*, 2006, **89**, 022906.
- 27 Q. N. Chen, S. B. Adler and J. Li, *Appl. Phys. Lett.*, 2014, **105**, 201602.
- 28 S. Hong, J. Woo, H. Shin, J. U. Jeon, Y. E. Pak, E. L. Colla, N. Setter, E. Kim and K. No, *J. Appl. Phys.*, 2001, **89**, 1377–1386.
- 29 A. Gannepalli, D. G. Yablou, A. H. Tsou and R. Proksch, *Nanotechnology*, 2011, **22**, 355705.
- 30 J. Woo, S. Hong, N. Setter, H. Shin, J.-U. Jeon, Y. E. Pak and K. No, *J. Vac. Sci. Technol. B*, 2001, **19**, 818.
- 31 E. Strelcov, Y. Kim, S. Jesse, Y. Cao, I. N. Ivanov, I. I. Kravchenko, C. H. Wang, Y. C. Teng, L. Q. Chen, Y. H. Chu and S. V. Kalinin, *Nano Lett.*, 2013, **13**, 3455–3462.
- 32 S. Jesse, N. Balke, E. Eliseev, A. Tselev, N. J. Dudney, A. N. Morozovska and S. V. Kalinin, *ACS Nano*, 2011, **5**, 9682–9695.

ChemComm

COMMUNICATION

A table of contents



The local strain change resulting from the proton redistribution and relaxation in Nafion could be visualized using electrochemical strain microscopy.